

Adaptive Data-Free Quantization

Biao Qian, Yang Wang*, Richang Hong, Meng Wang
 Key Laboratory of Knowledge Engineering with Big Data, Ministry of Education,
 School of Computer Science and Information Engineering,
 Hefei University of Technology, China

yangwang@hfut.edu.cn, {hfutqian, hongrc.hfut, eric.mengwang}@gmail.com

Abstract

Data-free quantization (DFQ) recovers the performance of quantized network (Q) without accessing the real data, but generates the fake sample via a generator (G) by learning from full-precision network (P) instead. However, such sample generation process is totally independent of Q , overlooking the adaptability of the knowledge from generated samples, i.e., informative or not to the learning process of Q , resulting into the overflow of generalization error. Building on this, several critical questions — how to measure the sample adaptability to Q under varied bit-width scenarios? how to generate the samples with large adaptability to improve Q 's generalization? whether the largest adaptability is the best? To answer the above questions, in this paper, we propose an Adaptive Data-Free Quantization (AdaDFQ) method, which reformulates DFQ as a zero-sum game upon the sample adaptability between two players — a generator and a quantized network. Following this viewpoint, we further define the disagreement and agreement samples to form two boundaries, where the margin is optimized to address the over-and-under fitting issues, so as to generate the samples with the desirable adaptability to Q . Our AdaDFQ reveals: 1) the largest adaptability is NOT the best for sample generation to benefit Q 's generalization; 2) the knowledge of the generated sample should not be informative to Q only, but also related to the category and distribution information of the training data for P . The theoretical and empirical analysis validate the advantages of AdaDFQ over the state-of-the-arts. Our code is available at <https://github.com/hfutqian/AdaDFQ>.

1. Introduction

Deep Neural Networks (DNNs) have encountered great challenges when involving the applications on resource-constrained devices, owing to the increasing demands for computing and storage resources. Network quantization [6, 10], which reduces the model size and energy consumption by mapping the floating-point weights and activations to low-bit ones, is a promising approach to improve the efficiency of DNNs. Quantization methods generally dedicate themselves to recovering the *performance drop* originating

*Yang Wang is the corresponding author.

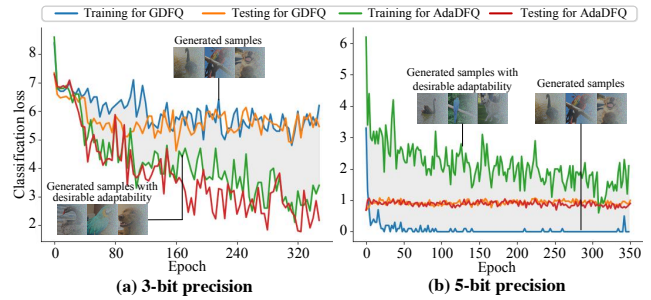


Figure 1. Existing work, e.g., GDFQ [21] (the blue), generally suffers from (a) underfitting issue (both training and testing loss are large) under 3-bit precision and (b) overfitting issue (training loss is small while testing loss is large) under 5-bit precision¹. Our AdaDFQ (the green) generates the sample with desirable adaptability to Q , yielding better generalization of Q with varied bit widths. The observations are from MobileNetV2 on ImageNet.

with the quantization errors, which involves fine-tuning or calibration operations with the original training data.

However, in many real-world scenes, such as medical and military fields, the original data may not be accessible due to privacy and security issues. Fortunately, recently proposed data-free quantization (DFQ), a potential method to quantize models without accessing the original data, aims to synthesize meaningful fake samples instead, which improves quantized network (Q) by knowledge distillation [5, 17] against the pre-trained full-precision model (P). Among the prior researches [1, 22], the generative fashions [3, 21, 24] have recently attracted increasing attention, owing to their superior performance. The generative model is introduced as a generator (G) to capture the distribution of the original data from P for better fake samples, where P is regarded as the discriminator to guide the generation process. For example, Qimera [3] generated boundary supporting samples to reduce the gap between the synthetic and real data. Nevertheless, *there still remains a non-ignorable performance loss when encountering various bit-width settings*. The reasons may lie in several aspects:

(1) Due to the limited capacity of the generator, the gen-

¹3-bit and 5-bit precision are representative for low-bit and high-bit cases, respectively, particularly: 3-bit quantization actually leads to a huge performance loss, which is a major challenge for the existing DFQ methods; while 5-bit or higher-bit quantization usually causes a small performance loss, which is selected to validate the generalization ability.

Table 1. Comparison with the existing DFQ methods. Our AdaDFQ aims to generate the sample with desirable adaptability to Q with varied bit widths, especially low-bit situation.

Method	Generated sample type	Dependence on Q	Access to low-bit situation
GDFQ [21]	Reconstructed	No	No
Qimera [3]	Reconstructed	No	No
ZAQ [11]	Adversarial	Yes	No
AdaDFQ	Adaptability-aware	Yes	Yes

erated sample with incomplete distribution is impossible to fully recover the original dataset, so that it is a crucial criterion: is the knowledge carried by the sample *informative* or not to the learning process of Q? However, in the existing arts, the generated sample customized for P, can't always benefit Q in varied bit-width settings (e.g., 3-bit or 5-bit precision, refer to (2)(3)), where only limited information from P can be utilized to recover Q.

- (2) In low-bit precision (e.g., 3 bit), Q often suffers from a sharp accuracy drop compared to P due to large quantization error, leading to its poor learning ability. Under such case, the generated sample by G may bring an unexpected large *disagreement* between the predictions of P and Q, which makes the optimization loss too large to converge, resulting in *underfitting* issue; see Fig.1(a).
- (3) In high-bit precision (e.g., 5 bit), Q still possesses comparable recognition ability with P due to a small accuracy drop. Under such case, most of the generated samples by G, for which Q and P give similar predictions (i.e., reach an *agreement*), may not benefit Q. However, under the constraint of the optimization loss, Q receives no improvement, even impairment, resulting in *overfitting* issue; see Fig.1(b).

Based on the above, the existing approaches fail to consider the *sample adaptability*, i.e., informative or not to Q, to Q with varied bit widths during the sample generation process from G, where Q is independent of the generation process; see Table 1. For example, for (2), the sample with large adaptability may be one with large agreement between P and Q; while for (3), it may be one with large disagreement. The above naturally elicits the following basic questions: *how to measure the sample adaptability to Q under varied bit-width scenarios?* *how to generate the samples with large adaptability to improve Q's generalization?* *whether the largest adaptability is the best?*

To answer the above questions, we propose an Adaptive Data-Free Quantization (AdaDFQ) method. Technically, we consider to generate the samples with large adaptability to Q by taking Q into account during the generation process; see Table 1. Specifically, G aims to generate the sample with *large* adaptability by enlarging the disagreement between P and Q, to benefit Q; while Q is calibrated to improve itself by exploiting the sample with large adaptability. It is apparent that such sample adaptability will not be large to Q after Q is refined; in other words, such process of benefiting Q leads to *decreasing* the sample adaptability, which

essentially *minimizes* the loss for Q, and is adversarial to maximizing the reward goal for G. Based on the above, anchored on sample adaptability, we reformulate DFQ as a dynamic zero-sum game process between two players — a generator and a quantized network, i.e., an adversarial game process where one player's reward is the other's loss while their sum is zero. Following the viewpoint, we further define two types of samples: disagreement (i.e., P can predict correctly but Q not) and agreement (i.e., P and Q have the same prediction) samples, to form the lower and upper boundaries to be balanced. The margin between the boundaries is optimized to address the over-and-under fitting issues, so as to generate the samples with the desirable adaptability to Q. We further conduct the theoretical analysis on the generalization of Q, which reveals: the generated sample with the largest adaptability is NOT the best for Q's generalization; the knowledge carried by the generated sample should not only be informative to Q, but also related to the category and distribution information of the training data for P.

We remark that AdaDFG is essentially an *adversarial* game governed by the sample adaptability, which is fundamentally orthogonal to the existing arts that improve Q by transferring knowledge from P to Q. One recent study [11] generates adversarial samples via G, by maximizing the gap between P and Q, and minimizing their gap to benefit Q for calibration. However, it fails to consider the sample adaptability to Q, hence suffers from the non-ideal generated samples. Besides, they focus primarily on the adversarial sample generation rather than adversarial game process perspective. The theoretical analysis and empirical studies validate the superiority of AdaDFG to the state-of-the-arts.

2. Adaptive Data-Free Quantization

Conventional generative data-free quantization (DFQ) methods [3, 21, 24] aim to reconstruct the training data with a generator (G) by exploiting the distribution from a pre-trained full-precision network (P), to help recover the performance of quantized network (Q) via the knowledge (i.e., the class distribution information about the training data from P) by the calibration operation. However, we observe that Q is independent of the generation process by the existing arts and whether the knowledge carried by generated samples is informative or not to Q, namely *sample adaptability*, is crucial to DFQ. To this end, we focus primarily on the sample adaptability to Q. Notably, DFQ is reformulated as a dynamic zero-sum game process governed by sample adaptability. To estimate the knowledge informativeness of the generated sample, one crucial question is how to measure the sample adaptability to Q, as discussed in the next.

2.1. How to Measure the Sample Adaptability to Quantized Network?

To measure the sample adaptability to Q, we focus primarily on following issues: 1) the *dependence* of generated sample on Q; 2) the *advantage* of P over Q in the generated sample; and 3) the *disagreement* between the predictions of P and Q, in that for Q with different bit widths (e.g., 3 or

5 bit), the disagreement varies greatly given the same sample to both P and Q. We define the generated sample that depends on Q, namely disagreement sample, as follows:

Definition 1 (Disagreement Sample). *Given a random noise vector $z \sim N(0, 1)$ and an arbitrary one-hot label y , a generator G generates a sample $x = G(z|y)$. Then the logit outputs of pre-trained full-precision model P and quantized model Q are given as $z_p = P(x)$ and $z_q = Q(x)$, respectively. Suppose that x can be correctly predicted by P , i.e., $\text{argmax}(z_p) = \text{argmax}(y)$, where $\text{argmax}(\cdot)$ returns the class index corresponding to maximum value. We determine x to be the disagreement sample provided $\text{argmax}(z_p) \neq \text{argmax}(z_q)$.*

Thus the probability vector encoding the disagreement between P and Q, is formulated as

$$p_{ds} = \text{softmax}(z_p - z_q) \in \mathbb{R}^C, \quad (1)$$

where C denotes the number of class; $p_{ds}(c) = \frac{\exp(z_p(c) - z_q(c))}{\sum_{j=1}^C \exp(z_p(j) - z_q(j))}$ ($c \in \{1, 2, \dots, C\}$) represents the c -th entry of the vector p_{ds} as the probability that x is labeled as the disagreement sample of the c -th class. Together with sample dependence to Q, disagreement sample can be viewed as the one with large adaptability to Q.

Another question is how to model the disagreement between P and Q, so as to measure the sample adaptability. Eq.(1) shows that the disagreement reaches the maximum provided the probability of c -th class $p_{ds}(c)$ approaches to 1 with other entries to be 0, which corresponds to the minimum entropy of p_{ds} ; while the disagreement reaches the minimum if each element in p_{ds} is equal (i.e., $z_p = z_q$), indicating the maximum entropy of p_{ds} . Hence, the disagreement can be calculated via the entropy of $\mathcal{H}_{info}(\cdot)$, and formulated as

$$\mathcal{H}_{info}(p_{ds}) = \sum_{c=1}^C p_{ds}(c) \log \frac{1}{p_{ds}(c)}. \quad (2)$$

For different datasets, C varies greatly, we further normalize $\mathcal{H}_{info}(p_{ds})$ as

$$\mathcal{H}_{nor} = 1 - \mathcal{H}'_{info}(p_{ds}) \in [0, 1], \quad (3)$$

where $\mathcal{H}'_{info}(p_{ds}) = \frac{\mathcal{H}_{info}(p_{ds}) - \min(\mathcal{H}_{info}(p_{ds}))}{\max(\mathcal{H}_{info}(p_{ds})) - \min(\mathcal{H}_{info}(p_{ds}))}$. The constant $\max(\mathcal{H}_{info}(p_{ds})) = -\sum_{c=1}^C \frac{1}{C} \log \frac{1}{C}$ represents the maximum value of $\mathcal{H}_{info}(p_{ds})$, where each element in p_{ds} has the same class probability $\frac{1}{C}$; Q perfectly aligns with P (i.e., $z_p = z_q$), while $\min(\cdot)$ represents the minimum value of $\mathcal{H}_{info}(p_{ds})$ within a batch. Thus, the sample adaptability is closely related to \mathcal{H}_{nor} — the more \mathcal{H}_{nor} is, the larger the disagreement over the sample to both P and Q is, leading to the larger sample adaptability.

As per Eq.(1)(3), $p_{ds} \in \mathbb{R}^C$ distributes in a C-dimensional vector space, while \mathcal{H}_{nor} is a real value. We hence map that to a C-dimensional space to characterize \mathcal{H}_{nor} via the unit vector $\frac{p_{ds}}{\|p_{ds}\|}$ ($\|\cdot\|$ denotes ℓ_2 norm), then \mathcal{H}_{nor} is reformulated as

$$\mathcal{H}_{nor}^C = \frac{p_{ds}}{\|p_{ds}\|} \mathcal{H}_{nor} = \frac{p_{ds}}{\|p_{ds}\|} (1 - \mathcal{H}'_{info}(p_{ds})) \in \mathbb{R}^C, \quad (4)$$

where the category information (i.e., $\frac{p_{ds}}{\|p_{ds}\|}$) of the generated sample apart from the disagreement (i.e., \mathcal{H}_{nor}) is exploited to well measure the sample adaptability.

The measurement of sample adaptability inspires us to revisit the DFQ: G aims to generate the sample with large adaptability to Q, equivalent to maximizing \mathcal{H}_{nor} (the gain of \mathcal{H}_{nor} is *positive*, serving as the reward for G), to benefit Q; while for the calibration process, Q is optimized to recover itself with the generated sample. It infers that such sample adaptability will not be large to Q, while the sample can no longer benefit Q after Q is refined, which results in decreasing the sample adaptability, and equivalent to minimizing \mathcal{H}_{nor} (the gain of \mathcal{H}_{nor} is *negative*, serving as the loss for G), *adversarial* to maximizing \mathcal{H}_{nor} , which encourages the loss for Q to cancel out the reward for G, such that the sum of reward and loss tends to be zero, such fact is in line with the principle of zero-sum game [19]¹, as discussed in the next section.

2.2. Zero-sum Game over Sample Adaptability

We formally revisit the DFQ as a zero-sum game between two players — a generator and a quantized network, as follows:

$$\min_{\theta_q \in \Theta_q} \max_{\theta_g \in \Theta_g} \mathcal{H}(\theta_g, \theta_q) = \min_{\theta_q \in \Theta_q} \max_{\theta_g \in \Theta_g} \mathbb{E}_{z,y} [1 - \mathcal{H}'_{info}(p_{ds})], \quad (5)$$

where G and Q are parameterized by $\theta_g \in \Theta_g$ and $\theta_q \in \Theta_q$, respectively. In particular, Eq.(5) is alternatively optimized via gradient descent during each iteration: on one hand, θ_q is fixed, the sample with *large* adaptability is generated by *maximizing* Eq.(5) to update θ_g , which *increases* the sample adaptability; on the other hand, θ_g is fixed, Q is calibrated over the generated sample by *minimizing* Eq.(5) to update θ_q , which benefits from *decreasing* the sample adaptability. During the zero-sum game, the overall changing (summation) of the sample adaptability to Q incurred by maximum and minimum optimization is close to zero. One critical question is how Eq.(5) converges to achieve the equilibrium (i.e., the sample adaptability no longer changes) for the zero-sum game. Thanks to the classical Nash equilibrium [2], where no player can improve its individual gain during the zero-sum game, the optimization process will reach an equilibrium (θ_g^*, θ_q^*) when (1) fixing θ_q^* , G fails to maximize $\mathcal{H}(\theta_g, \theta_q^*)$ to obtain a $\theta_g \in \Theta_g$, yielding $\mathcal{H}(\theta_g, \theta_q^*) > \mathcal{H}(\theta_g^*, \theta_q^*)$; (2) fixing θ_g^* , Q can no longer improve itself by minimizing $\mathcal{H}(\theta_g^*, \theta_q)$ to obtain a $\theta_q \in \Theta_q$, yielding $\mathcal{H}(\theta_g^*, \theta_q) < \mathcal{H}(\theta_g^*, \theta_q^*)$. Based on that, for all $\theta_g \in \Theta_g$ and $\theta_q \in \Theta_q$, (θ_g^*, θ_q^*) meets the following:

$$\mathcal{H}(\theta_g, \theta_q^*) \leq \mathcal{H}(\theta_g^*, \theta_q^*) \leq \mathcal{H}(\theta_g^*, \theta_q), \quad (6)$$

where θ_g^* and θ_q^* are the parameters of G and Q under an equilibrium state, respectively. Maximizing Eq.(5) is equivalent to maximizing $\mathcal{H}(\cdot, \cdot)$ throughout learning G to

¹ For AdaDFQ, G aims to enlarge the disagreement, i.e., adaptability to Q, between P and Q, while Q decreases it by learning from P, where they cancel each other out, making the overall changing (summation) of the disagreement ($\mathcal{H}_{info}(p_{ds})$) *close* to 0 (see Fig.3 for such intuition), which is consistent to the intuition of zero-sum game.

generate the sample with largest adaptability (*i.e.*, smallest $\mathcal{H}'_{info}(p_{ds})$). However, such fact may incur:

Underfitting issue: the knowledge carried by the generated samples from G (*e.g.*,  in Fig.2), exhibits excessive information with large adaptability, implying a large disagreement between P and Q, while Q (especially for Q with low bit width) has no sufficient ability to learn informative knowledge from P. Evidently, the sample with the largest adaptability (*i.e.*, smallest $\mathcal{H}'_{info}(p_{ds})$) is not the best. For such case, Q is calibrated by minimizing Eq.(5) over such samples to incur the underfitting, which, in turn, encourages G to generate the samples with lower adaptability (*i.e.*, larger $\mathcal{H}'_{info}(p_{ds})$) by alternatively maximizing Eq.(5). However, encouraging the sample with lowest adaptability (*i.e.*, largest $\mathcal{H}'_{info}(p_{ds})$) may lead to:

Overfitting issue: the knowledge carried by the generated samples (*e.g.*,  in Fig.2) delivers limited information with small adaptability to yield a large agreement between P and Q. For such case, it may not be informative to calibrate Q (especially for Q with high bit width) by minimizing Eq.(5), which alternatively encourages G to generate the samples with the larger adaptability by maximizing Eq.(5).

2.3. Refining the Maximization of Eq.(5): Generating the Sample with Desirable Adaptability

The above facts indicate that the sample with either largest or lowest adaptability generated by maximizing Eq.(5) is not necessarily the best, incurring over-and-under fitting issues, which fail to be resolved by the above disagreement sample (Definition 1) since it focuses on the larger adaptability (*i.e.*, smaller $\mathcal{H}'_{info}(p_{ds})$). To address the issues, we refine the maximization of Eq.(5) during the zero-sum game by proposing to balance disagreement sample with agreement sample, as discussed in the next.

2.3.1 Balancing Disagreement Sample with Agreement Sample

As per Definition 1, the category (label) information from P is crucial to establish the dependence of generated sample to Q. Hence, to generate the disagreement sample with desirable adaptability, we exploit the category (label) information to guide G for sample generation. Given the label y , it is expected that the generated sample is classified as disagreement sample with the same label y . Thereby, we present the following Cross-Entropy loss $\mathcal{H}_{CE}(\cdot, \cdot)$ to match p_{ds} and y :

$$\mathcal{L}_{ds} = \mathbb{E}_{z,y}[\mathcal{H}_{CE}(p_{ds}, y)]. \quad (7)$$

Eq.(7) encourages G to generate the disagreement sample that P can predict correctly but Q fails. However, the disagreement sample tends to yield smaller $\mathcal{H}'_{info}(p_{ds})$, which mitigates the overfitting while the underfitting issue is still available. To remedy such issue, we further define the agreement sample to weaken the effect of disagreement sample on reducing $\mathcal{H}'_{info}(p_{ds})$.

Definition 2 (Agreement Sample). *Based on Definition 1, we say the generated sample x is the agreement sample if $\text{argmax}(z_p) = \text{argmax}(z_q)$.*

Thus, similar in spirit to p_{ds} , the probability vector that describes the agreement between P and Q, is formulated as

$$p_{as} = \text{softmax}(z_p + z_q) \in \mathbb{R}^C, \quad (8)$$

where $p_{as}(c) = \frac{\exp(z_p(c) + z_q(c))}{\sum_{j=1}^C \exp(z_p(j) + z_q(j))}$ is the c -th entry of the vector p_{as} as the probability that x is the agreement sample of the c -th class. Following Eq.(7), p_{as} and y are matched via the following loss function:

$$\mathcal{L}_{as} = \mathbb{E}_{z,y}[\mathcal{H}_{CE}(p_{as}, y)]. \quad (9)$$

Eq.(9) encourages G to generate the agreement sample that both P and Q can correctly predict to possess larger $\mathcal{H}'_{info}(p_{ds})$. Intuitively, the agreement sample is capable of balancing disagreement sample to avoid too small or large $\mathcal{H}'_{info}(p_{ds})$ for desirable adaptability, and formulated as

$$\mathcal{L}_{bal} = \alpha_{ds}\mathcal{L}_{ds} + \alpha_{as}\mathcal{L}_{as}, \quad (10)$$

where α_{ds} and α_{as} are used to facilitate the balance between \mathcal{L}_{ds} and \mathcal{L}_{as} (see the parameter study). Eq.(10) denotes the loss between p_{ds} , p_{as} and y to be minimized during the training phase. From this perspective, \mathcal{L}_{ds} attempts to generate the disagreement samples to enlarge the gap between P and Q, so as to reduce $\mathcal{H}'_{info}(p_{ds})$ for agreement samples (see  in Fig.2); to be analogous, \mathcal{L}_{as} enlarges $\mathcal{H}'_{info}(p_{ds})$ for disagreement samples (see  in Fig.2).

Intuitively, \mathcal{L}_{bal} endows the generated sample with the desirable adaptability, *i.e.*, neither too large nor small $\mathcal{H}'_{info}(p_{ds})$ for the generated samples throughout the balance between disagreement and agreement samples. In other words, we need to study how to control $\mathcal{H}'_{info}(p_{ds})$ *within a desirable range* via the balance process; cored on that, it establishes the implicit lower and upper boundary corresponding to the disagreement and agreement samples (see Fig.2), hence the above curse is equivalent to confirming the margin between such lower-and-upper boundary. To this end, we propose to optimize the margin between these two boundaries, as discussed in the next.

2.3.2 Optimizing the Margin Between two Boundaries

Formally, along with \mathcal{L}_{bal} , the maximization objective of Eq.(5) is imposed with the desirable bound constraints for $\mathcal{H}'_{info}(p_{ds})$ (see Fig.2), and formulated as

$$\begin{aligned} & \max_{\theta_g \in \Theta_g} \mathcal{H}(\theta_g, \theta_q) - \beta \mathcal{L}_{bal}, \\ & \text{subject to } \lambda_l < \mathcal{H}'_{info}(p_{ds}) < \lambda_u, \end{aligned} \quad (11)$$

where β is utilized to balance the agreement and disagreement sample. λ_l and λ_u denote the lower and upper bound of $\mathcal{H}'_{info}(p_{ds})$, such that $0 \leq \lambda_l < \lambda_u \leq 1$. where the goal is to ensure the balance process to generate the sample with

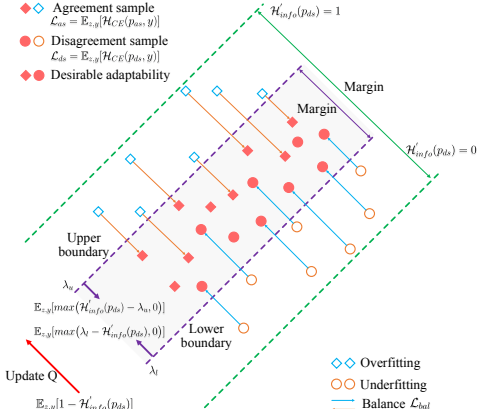


Figure 2. Illustration of generating the sample with desirable adaptability to address the over-and-under fitting issues.

desirable adaptability. λ_l serves to prevent G from generating the sample with too large adaptability (*i.e.*, too small $\mathcal{H}'_{info}(p_{ds})$) via maximizing Eq.(5), where Q is calibrated by minimizing Eq.(5) to incur *underfitting*. By contrast, λ_u aims to avoid the sample with too small adaptability (*i.e.*, too large $\mathcal{H}'_{info}(p_{ds})$), which is not informative to calibrate Q by minimizing Eq.(5), causing *overfitting* issue.

Discussion on λ_l and λ_u . The crucial issue is how to specify λ_l and λ_u ? First, we investigate the ideal condition where Q can be well calibrated over varied generated samples from G, it is ideally expected that each generated sample possesses an optimal pairwise of λ_l and λ_u , to help calibrate Q by minimizing Eq.(5), which, unfortunately, is infeasible for individual sample since a large number of generated samples within a batch are generated from G to calibrate Q, only single sample makes no sense; for each batch, the adaptability of each single sample is merely affected by its preceding generated sample, and independent of all other generated samples from G; worse still, the dependencies between varied batches are quite uncertain, since Q varies after being calibrated for each batch. As inspired, instead of trapping into the adaptive rule to each individual sample, we propose to acquire the range of λ_l and λ_u for all generated samples. Particularly, we uniformly select the values of λ_l and λ_u for all samples from $[0, 1]$ (see the extensive parameter study), to answer “how much” to the balancing process (Eq.(10)), such that the following demands meet. That is, avoiding too small λ_l or large λ_u , to address the over-and-under fitting issues, so as to ensure G to well generate the samples with desirable adaptability.

The above fact discussed the adaptability of single sample to Q, while calibrating Q requires the generated samples within a batch, motivating us to exploit the distribution of the training data for better generalization. We consider the batch normalization statistics (BNS) information [3, 21] about the training data for P, which is learned by

$$\mathcal{L}_{BNS} = \sum_{m=1}^M (\|\mu_m^g - \mu_m\|_2^2 + \|\sigma_m^g - \sigma_m\|_2^2), \quad (12)$$

where μ_m^g/σ_m^g and μ_m/σ_m denote the mean/variance of the generated sample’s distribution within a batch and the corresponding mean/variance parameters for P at the m -th

BN layer of the total M layers. Eq.(12) encodes the loss between them to be minimized during the training. To this end, the maximization objective of Eq.(5) is refined as

$$\begin{aligned} & \max_{\theta_g \in \Theta_g} \mathbb{E}_{z,y}[-\max(\lambda_l - \mathcal{H}'_{info}(p_{ds}), 0)] \\ & \mathbb{E}_{z,y}[-\max(\mathcal{H}'_{info}(p_{ds}) - \lambda_u, 0)] - \beta \mathcal{L}_{bal} - \gamma \mathcal{L}_{BNS}, \end{aligned} \quad (13)$$

where the first two terms aim to optimize the margin between λ_l and λ_u via the hinge loss [9]. $\max(\cdot, \cdot)$ returns the maximum. β and γ are balance parameters, where, the minus “-” for \mathcal{L}_{bal} and \mathcal{L}_{BNS} is noted to be minimized during the optimization as aforementioned. With Eq.(13), the minimization objective of Eq.(5) holds to calibrate Q for performance recovery, yielding:

$$\min_{\theta_q \in \Theta_q} \mathbb{E}_{z,y}[1 - \mathcal{H}'_{info}(p_{ds})]. \quad (14)$$

By alternatively optimizing Eq.(13) and (14) during a zero-sum game, the samples with desirable adaptability can be generated by G to maximally recover the performance of Q until reaching a Nash equilibrium.

2.4. Theoretical Analysis: Why do the Boundaries Improve Q’s Generalization?

One may wonder why AdaDFQ can generate the sample with desirable adaptability. We answer the question by studying the generalization of Q trained on the generated samples from a statistic view. According to the VC theory [12, 13, 20], the classification error of a quantized network (Q) learning from the ground truth label (y) on the generated samples by G can be decomposed as

$$R(f_q) - R(f_r) \leq O\left(\frac{|\mathcal{F}_q|_C}{n^{\alpha_{qr}}}\right) + \varepsilon_{qr}, \quad (15)$$

where $R(\cdot)$ is the error of a specific function. $f_q \in \mathcal{F}_q$ is the quantized network (Q) function and $f_r \in \mathcal{F}_r$ is the ground truth label (y) function. ε_{qr} denotes the approximation error of the quantized network function class \mathcal{F}_q (considering all possible acquired f_q by optimizing Q w.r.t. $f_r \in \mathcal{F}_r$ (a fixed learning target) on the generated samples during the training phase. α_{qr} denotes the learning rate for the given generated samples, particularly: when α_{qr} approaches $\frac{1}{2}$ (a slow rate) for the generated samples with the excessive information to Q; while approaching 1 (a fast rate) for the generated samples with the limited information to Q. $O(\cdot)$ represents the estimation error of a network function over the real data during the testing phase. $|\cdot|_C$ measures the capacity of a function class and n is the number of the generated samples from G. Similarly, let $f_p \in \mathcal{F}_p$ be the full-precision network (P) function, then

$$R(f_p) - R(f_r) \leq O\left(\frac{|\mathcal{F}_p|_C}{n^{\alpha_{pr}}}\right) + \varepsilon_{pr}, \quad (16)$$

where α_{pr} is related to the learning rate of P upon the ground truth label (y); ε_{pr} denotes the approximation error of the full-precision network (P) function class \mathcal{F}_p w.r.t. $f_r \in \mathcal{F}_r$. For data-free setting, Q is required to learn from P with the generated samples, which yields the following:

$$R(f_q) - R(f_p) \leq O\left(\frac{|\mathcal{F}_q|_C}{n^{\alpha_{qp}}}\right) + \varepsilon_{qp}, \quad (17)$$

where α_{qp} is related to the learning rate of Q upon P, while ε_{qp} is the approximation error of the quantized network (Q) function class \mathcal{F}_q w.r.t. $f_p \in \mathcal{F}_p$. For such case, to study the classification error of Q learning from the ground truth label y on the generated samples, we combine Eq.(16) and (17) [12, 13], leading to

$$\begin{aligned} R(f_q) - R(f_r) &= R(f_q) - R(f_p) + R(f_p) - R(f_r) \\ &\leq O\left(\frac{|\mathcal{F}_q|_C}{n^{\alpha_{qp}}}\right) + \varepsilon_{qp} + O\left(\frac{|\mathcal{F}_p|_C}{n^{\alpha_{pr}}}\right) + \varepsilon_{pr} \\ &= O\left(\frac{|\mathcal{F}_q|_C}{n^{\alpha_{qp}}}\right) + O\left(\frac{|\mathcal{F}_p|_C}{n^{\alpha_{pr}}}\right) + \underbrace{\varepsilon_{qp} + \varepsilon_{pr}}_{\text{Estimation error}} + \underbrace{\varepsilon_{qp} + \varepsilon_{pr}}_{\text{Approximation error}} \end{aligned} \quad (18)$$

Evidently, Eq.(18) shows that, to benefit the generalization of Q, both estimation and approximation error should be reduced, so that a tighter upper bound can be captured, where we claim that to be consistent with the insights on the optimization of Eq.(13): *first*, as aforementioned, the reasons for the overflow of generalization error stem from: 1) the generated sample with too large $\mathcal{H}'_{info}(p_{ds})$ is not informative to calibrate Q, *i.e.*, the small ε_{qp} during the training stage and large $O\left(\frac{|\mathcal{F}_q|_C}{n^{\alpha_{qp}}}\right)$ during the testing stage, leading to *overfitting* issue for Q; 2) for the generated sample with too small $\mathcal{H}'_{info}(p_{ds})$, Q has no sufficient ability to learn informative knowledge from P, *i.e.*, both ε_{qp} during the training stage and $O\left(\frac{|\mathcal{F}_q|_C}{n^{\alpha_{qp}}}\right)$ during the testing stage are large, leading to *underfitting* issue for Q. Based on that, λ_l and λ_u in Eq.(11) along with the balance process (\mathcal{L}_{bal}) in Eq.(10) aim to avoid too large or small ε_{qp} by optimizing the margin, thus the estimation error $O\left(\frac{|\mathcal{F}_q|_C}{n^{\alpha_{qp}}}\right)$ can be reduced, *i.e.*, overcoming the *over-and-under fitting* issues. *Second*, the above fact discussed the adaptability of single sample to Q, as aforementioned, BNS distribution information (Eq.(12)) of the training data extracted from P further facilitates calibrating Q for better generalization via the generated samples within a batch, which ensures the generated samples to be informative to P, *i.e.*, decreasing $O\left(\frac{|\mathcal{F}_p|_C}{n^{\alpha_{pr}}}\right) + \varepsilon_{pr}$ in Eq.(16) or (18), along with the category information from P regarding the disagreement and agreement samples.

Based on the above, the sample with desirable adaptability to Q can be generated by optimizing Eq.(13), reducing both estimation and approximation error (obtaining a tighter upper bound) in Eq.(18), so as to generate the samples by G with desirable adaptability which is beneficial to calibrating Q for better generalization by optimizing Eq.(14), where they are alternatively optimized during a zero-sum game until reaching a Nash equilibrium.

3. Experiment

3.1. Experimental Settings and Details

We validate AdaDFQ over three typical image classification datasets, *i.e.*, **CIFAR-10**, **CIFAR-100** [8] and **ImageNet (ILSVRC2012)** [18]. CIFAR-10 and CIFAR-100 contain 10 and 100 classes of images. Both of them are split into 50K training images and 10K testing images. ImageNet consists of 1.2M samples for training and 50k samples for validation with 1000 categories. For data-free set-

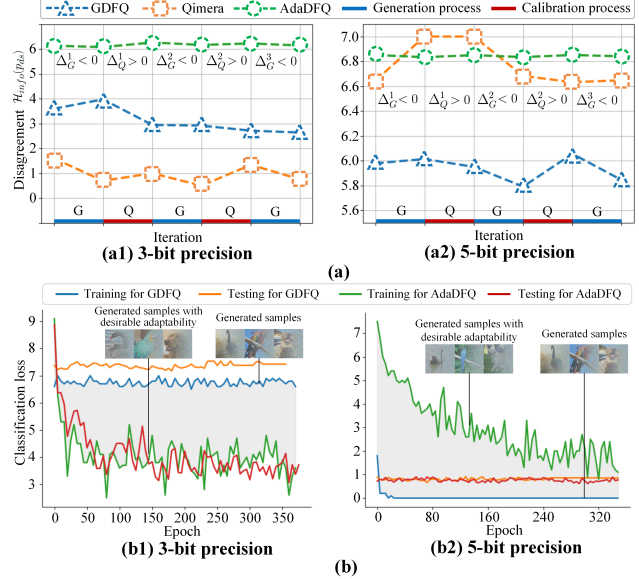


Figure 3. Illustration of AdaDFQ on generating the samples with desirable adaptability to Q under 3-bit and 5-bit precision. (a) Disagreement between P and Q during the generation (—) and calibration (—) process. $\Delta_Q^i > 0$ and $\Delta_G^i < 0$ denote the positive and negative gain of the disagreement, *i.e.*, $\mathcal{H}_{info}(p_{ds})$, at i -th iteration of zero-sum game for the sample generation from G and calibration to Q. (b) Classification loss for Q during the training and testing phases.

ting, only validation sets are adopted to evaluate the performance of the quantized models Q. We quantize pre-trained full-precision networks P including ResNet-20 for CIFAR, and ResNet-18, ResNet-50, and MobileNetV2 for ImageNet, via the following quantizers to yield Q:

Quantizer. Following [3, 21], we quantize both full-precision (float32) weights and activations into n -bit precision by a symmetric linear quantization method as [6]:

$$\theta_q = \text{round}\left((2^n - 1) * \frac{\theta - \theta_{min}}{\theta_{max} - \theta_{min}} - 2^{n-1}\right), \quad (19)$$

where θ and θ_q are the full-precision and quantized value. $\text{round}(\cdot)$ returns the nearest integer value to the input. θ_{min} and θ_{max} are the minimum and maximum of θ .

For *generation* process, we construct the architecture of the generator G following ACGAN [15], which is trained via Eq.(13) using Adam [7] as an optimizer with a momentum of 0.9 and a learning rate of 1e-3. For *calibration* process, Q is optimized by minimizing Eq.(14), where SGD with Nesterov [14] is adopted as an optimizer with a momentum of 0.9 and weight decay of 1e-4. For CIFAR, the learning rate is initialized to 1e-4 and decayed by 0.1 for every 100 epochs, while it is 1e-5 for ImageNet. G and Q are alternatively trained for 400 epochs. The batch size is set to 16. For hyper-parameters, α_{ds} and α_{as} in Eq.(10); λ_l , λ_u , β and γ in Eq.(13) are empirically set to 0.2, 0.1, 0.1, 0.8, 1 and 1. (see our supplementary material for more parameter studies). All experiments are implemented with pytorch [16] via the code of GDFQ [21] and run on an NVIDIA GeForce GTX 1080 Ti GPU and an Intel(R) Core(TM) i7-6950X CPU @ 3.00GHz.

Table 2. Accuracy (%) comparison with the state-of-the-arts on CIFAR-10, CIFAR-100 and ImageNet. \dagger : the results implemented by author-provided code. -: no results are reported. $nwna$ indicates the weights and activations are quantized to n -bit. The best results are reported with **boldface**.

Dataset	Model (Full precision)	Bit width	ZAQ [11] (CVPR 2021)	IntraQ [23] (CVPR 2022)	ARC+AIT [4] (CVPR 2022)	GDFQ [21] (ECCV 2020)	ARC [24] (IJCAI 2021)	Qimera [3] (NeurIPS 2021)	AdaDFQ (Ours)
CIFAR-10	ResNet-20 (93.89)	3w3a	-	77.07	-	75.11 \dagger	-	74.43 \dagger	84.89
		4w4a	92.13	91.49	90.49	90.11	88.55	91.26	92.31
		5w5a	93.36	-	92.98	93.38	92.88	93.46	93.81
CIFAR-100	ResNet-20 (70.33)	3w3a	-	48.25	41.34	47.61 \dagger	40.15	46.13 \dagger	52.74
		4w4a	60.42	64.98	61.05	63.75	62.76	65.10	66.81
		5w5a	68.70	-	68.40	67.52	68.40	69.02	69.93
ImageNet	ResNet-18 (71.47)	3w3a	-	-	-	20.23 \dagger	23.37	1.17 \dagger	38.10
		4w4a	52.64	66.47	65.73	60.60	61.32	63.84	66.53
		5w5a	64.54	69.94	70.28	68.49	68.88	69.29	70.29
	MobileNetV2 (73.03)	3w3a	-	-	-	1.46 \dagger	14.30	-	28.99
		4w4a	0.10	65.10	66.47	59.43	60.13	61.62	65.41
		5w5a	62.35	71.28	71.96	68.11	68.40	70.45	71.61
	ResNet-50 (77.73)	3w3a	-	-	-	0.31 \dagger	1.63	-	17.63
		4w4a	53.02	-	68.27	54.16	64.37	66.25	68.38
		5w5a	73.38	-	76.00	71.63	74.13	75.32	76.03

Table 3. Ablation study about varied components of AdaDFQ on ImageNet. $nwna$ indicates the weights and activations are quantized to n -bit. The best results are reported with **boldface**.

Model (Full-precision)	\mathcal{L}_{ds}	\mathcal{L}_{as}	λ_l, λ_u	\mathcal{L}_{BNS}	3w3a	5w5a
ResNet-18 (71.47)	✓	✓	✓	✓	14.86	69.15
	✓	✓	✓	✓	26.41	69.81
	✓	✓	✓	✓	15.01	70.06
	✓	✓	✓	✓	32.52	70.13
	✓	✓	✓	✓	20.98	67.35
	✓	✓	✓	✓	38.10	70.29

To validate how AdaDFQ generates the sample with desirable adaptability, we empirically validate “why” AdaDFQ works, including the comparisons with the state-of-the-arts, ablation study as well as visual analysis.

3.2. Why does AdaDFQ Work?

We verify the core idea of AdaDFQ — generating the sample with desirable adaptability to yield better Q’s generalization with varied bit widths. We perform the experiments with ResNet-18 (Fig.3 (a)) and ResNet-50 (Fig.3 (b)) serving as both P and Q on ImageNet. Fig.3(a) illustrates that, compared to GDFQ [21] and Qimera [3], the disagreement (computed by Eq.(2)) between P and Q for AdaDFQ performs stably within a small range, *i.e.*, the overall changing summation ($\Delta_G^i + \Delta_Q^i$) of the disagreement is *close* to 0, following the principle of zero-sum game (Sec.2.2), which confirms that the generated sample with desirable adaptability by AdaDFQ is fully exploited to benefit Q, and the lower and upper bound constraints (λ_l and λ_u in Eq.(13)) avoid generating the sample with too large or small adaptability, which leads to ridiculously large disagreement or agreement. Fig.3(b) reveals that AdaDFQ achieves better Q’s generalization with 3-bit and 5-bit precision unlike GDFQ, where the generated sample with desirable adaptability succeeds in overcoming the *underfitting* (both training and testing loss are large) and *overfitting* (small training loss but large testing loss), confirming the analysis in Sec.2.4.

3.3. Comparison with State-of-the-arts

To verify the superiority of AdaDFG, we compare it with typical DFQ methods, *i.e.*, GDFQ [21], ARC [24] and

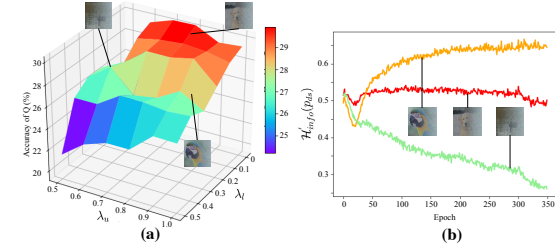


Figure 4. Ablation study about λ_l and λ_u , (a) Accuracy (%) comparison of Q with varied (λ_l, λ_u) . (b) $\mathcal{H}_{info}(p_{ds})$ for the generated samples corresponding to different areas in (a).

Qimera [3]: reconstructing the original data from P; **ZAQ** [11] focuses primarily on the adversarial sample generation rather than adversarial game process for AdaDFG; **IntraQ** [23] optimizes the noise to obtain fake sample without a generator; **AIT** [4] improves the loss function and gradients for ARC to generate better sample, denoted as **ARC+AIT**.

Table 2 summarizes our following findings: 1) AdaDFQ offers a significant and consistent performance gain over the state-of-the-arts, in line with our purpose of generating the sample with desirable adaptability to Q in Sec.2.3. Impressively, AdaDFQ achieves at most 10.46%, 6.61% and 36.93% accuracy gains on CIFAR-10, CIFAR-100 and ImageNet. Notably, compared with GDFQ, ARC and Qimera where Q is independent of the generation process, AdaDFQ obtains accuracy improvement with a large margin, *e.g.*, at least 0.35% gain (ResNet-20 with 5w5a on CIFAR-10), confirming the necessity of AdaDFQ over the sample adaptability to Q in Sec.1. Specifically, ZAQ suffers from a large performance gap compared to AdaDFQ, since many unexpected samples are generated without considering the sample adaptability, which is harmful to calibrating Q. AdaDFQ outperforms AIT despite of the combination with ARC. 2) AdaDFQ achieves the substantial gains for Q under varied bit-widths, confirming the importance of desirable adaptability to varied Q (Sec.2.3). Note that, especially for 3-bit case, most of the existing arts suffer from a poor accuracy, even fail to converge, while AdaDFQ obtains at most 36.93% (ResNet-18 with 3w3a) and at least 4.49% (ResNet-20 with 3w3a on CIFAR-100) performance gains.

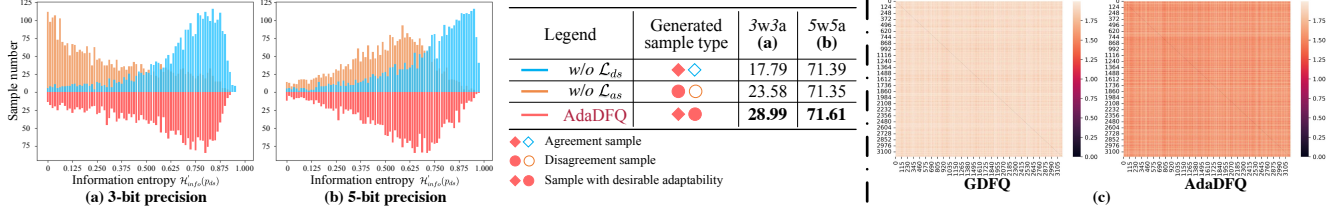


Figure 5. (a)(b) Illustration of how to balance \mathcal{L}_{ds} and \mathcal{L}_{as} to generate the sample with desirable adaptability under 3-bit and 5-bit precision. (c) Visual analysis: the similarity comparison between the generated samples.

3.4. Ablation Study

3.4.1 Validating adaptability with disagreement and agreement samples

As aforementioned, the disagreement and agreement samples play a critical role in addressing the over-and-under fitting issues for the desirable adaptability. We conduct the ablation study on \mathcal{L}_{ds} (Eq.(7)) and \mathcal{L}_{as} (Eq.(9)) over ImageNet. Table 3 suggests the great superiority (38.10%, 70.29%) of AdaDFQ (including the both) over other cases. Note that, removing either or both of \mathcal{L}_{ds} and \mathcal{L}_{as} obtains a large accuracy loss (at most 23.24% and 1.14%), implying the intuition of balancing the disagreement sample with agreement sample (Sec.2.3.1). Interestingly, the case without λ_l and λ_u (Eq.(13)) receives the minimal accuracy loss (5.58% and 0.16%), confirming the importance of the bound constraints on the basis of \mathcal{L}_{bal} (Eq.(10)).

3.4.2 Why can λ_l and λ_u benefit Q?

The parameters λ_l and λ_u in Eq.(13) serve as a lower and upper bound of the desirable adaptability (neither too small or large $\mathcal{H}'_{info}(p_{ds})$) for the sample generation, which is critical to address the over-and-under fitting issues. We aim to verify the effectiveness of varied parameter configurations ($\lambda_l \in \{0, 0.1, 0.2, 0.3, 0.4, 0.5\}$, $\lambda_u \in \{0.5, 0.6, 0.7, 0.8, 0.9, 1.0\}$) via the grid search and perform the experiments under 3-bit precision with MobileNetV2 serving as P and Q on ImageNet. Fig.4(a) illustrates that AdaDFQ achieves the significant performance within an optimal range (the red area in Fig.4(a)), *i.e.*, $\lambda_l \in \{0, 0.1, 0.2\}$ and $\lambda_u \in \{0.7, 0.8, 0.9\}$, indicating a wide range between two bounds, where the performance of Q is insensitive to λ_l and λ_u , which offers a guideline for the selection of their values (λ_l and λ_u is set to 0.1, 0.8 in the main experiments), verifying the feasibility to uniformly select the values of λ_l and λ_u for all samples (Sec.2.3.2). Besides, Fig.4(b) provides evidence that λ_l and λ_u within the optimal range contributes to yielding the desirable adaptability, where $\mathcal{H}'_{info}(p_{ds})$ (the red in Fig.4(b)) is neither too small (the green in Fig.4(b)) or large (the orange in Fig.4(b)).

3.4.3 How to balance disagreement sample with agreement sample?

We further study the effectiveness of \mathcal{L}_{bal} in Eq.(10), and how to balance disagreement sample with agreement sample via two cases: **A**: only generating disagreement sample, denoted as *w/o* \mathcal{L}_{as} ; and **B**: only generating agree-

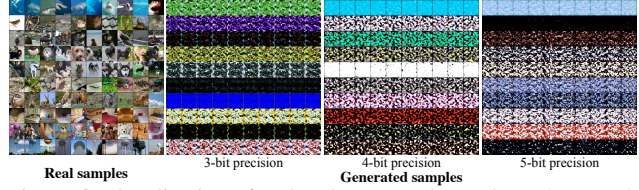


Figure 6. Visualization of real and generated samples, where each row denotes one of 10 randomly chosen classes from ImageNet.

ment sample, denoted as *w/o* \mathcal{L}_{ds} . We perform the experiments and generate 3200 samples under 3-bit and 5-bit precision with MobileNetV2 serving as P and Q on ImageNet. Fig.5(a)(b) illustrates that most of the generated samples (— in Fig.5(a)(b)) from case A yield smaller $\mathcal{H}'_{info}(p_{ds})$ than those (— in Fig.5(a)(b)) from case B, which provides a basis for balancing \mathcal{L}_{ds} with \mathcal{L}_{as} . It is observed that $\mathcal{H}'_{info}(p_{ds})$ of the generated sample (— in Fig.5(a)(b)) from AdaDFQ is neither too small nor large compared to case A and B, which is evidence that \mathcal{L}_{bal} forces the disagreement and agreement samples to move towards each other between two boundaries, in line with the analysis in Sec.2.3.1.

3.5. Visual Analysis on Generated Samples

To further show the desirable adaptability of the generated samples by AdaDFQ to Q, we conduct the visual analysis over MobileNetV2 serving as both P and Q on ImageNet by the similarity matrix (each element is obtained by computing the ℓ_1 norm between the probability distribution p_{ds} of every two samples), along with the visualization of generated samples (10 images per category) from 10 categories. Fig.5(c) illustrates that the generated samples by AdaDFQ possess a much larger similarity (the darker, the larger) than those by GDFQ [21], implying that the generated sample by GDFQ varies greatly, where substantial samples with low adaptability exist against AdaDFQ. Fig.6 shows that the generated samples for different bit widths (*i.e.*, 3 bit, 4 bit and 5bit) vary greatly, confirming the intuition of AdaDFQ — generating the sample with desirable adaptability to varied Q (Sec.2.3); while the samples from varied categories differ greatly from each other, confirming that the category information is fully exploited (Sec.2.3.1); *due to page limitation, see more results with higher resolution in supplementary material.*

4. Conclusion

In this paper, we propose an Adaptive Data-Free Quantization (AdaDFQ) method, which formulates the DFQ as a zero-sum game process between two players. Following

the viewpoint, the disagreement and agreement samples are further defined to form the lower and upper boundaries. The margin between two boundaries is optimized to address the over-and-under fitting issues, so as to generate the samples with the desirable adaptability to calibrate Q. The theoretical analysis and empirical studies validate the advantages of AdaDFQ to the existing arts.

5. Acknowledgments

This work are supported by National Natural Science Foundation of China under the grant no U21A20470, 62172136, 72188101, U1936217. Key Research and Technology Development Projects of Anhui Province (no.202004a5020043).

References

- [1] Yaohui Cai, Zhewei Yao, Zhen Dong, Amir Gholami, Michael W Mahoney, and Kurt Keutzer. Zeroq: A novel zero shot quantization framework. In *Proceedings of the IEEE/CVF Conference on Computer Vision and Pattern Recognition*, pages 13169–13178, 2020. [1](#)
- [2] Adrian Rivera Cardoso, Jacob Abernethy, He Wang, and Huan Xu. Competing against nash equilibria in adversarially changing zero-sum games. In *International Conference on Machine Learning*, pages 921–930. PMLR, 2019. [3](#)
- [3] Kanghyun Choi, Deokki Hong, Noseong Park, Youngsok Kim, and Jinho Lee. Qimera: Data-free quantization with synthetic boundary supporting samples. *Advances in Neural Information Processing Systems*, 34, 2021. [1, 2, 5, 6, 7](#)
- [4] Kanghyun Choi, Hye Yoon Lee, Deokki Hong, Joonsang Yu, Noseong Park, Youngsok Kim, and Jinho Lee. It’s all in the teacher: Zero-shot quantization brought closer to the teacher. In *Proceedings of the IEEE/CVF Conference on Computer Vision and Pattern Recognition*, pages 8311–8321, 2022. [7](#)
- [5] Geoffrey Hinton, Oriol Vinyals, and Jeff Dean. Distilling the knowledge in a neural network. In *NIPS*, 2015. [1](#)
- [6] Benoit Jacob, Skirmantas Kligys, Bo Chen, Menglong Zhu, Matthew Tang, Andrew Howard, Hartwig Adam, and Dmitry Kalenichenko. Quantization and training of neural networks for efficient integer-arithmetic-only inference. In *Proceedings of the IEEE conference on computer vision and pattern recognition*, pages 2704–2713, 2018. [1, 6](#)
- [7] Diederik P Kingma and Jimmy Ba. Adam: A method for stochastic optimization. *arXiv preprint arXiv:1412.6980*, 2014. [6](#)
- [8] Alex Krizhevsky, Geoffrey Hinton, et al. Learning multiple layers of features from tiny images. 2009. [6](#)
- [9] Jae Hyun Lim and Jong Chul Ye. Geometric gan. *arXiv preprint arXiv:1705.02894*, 2017. [5](#)
- [10] Darryl Lin, Sachin Talathi, and Sreekanth Annapureddy. Fixed point quantization of deep convolutional networks. In *International conference on machine learning*, pages 2849–2858. PMLR, 2016. [1](#)
- [11] Yuang Liu, Wei Zhang, and Jun Wang. Zero-shot adversarial quantization. In *Proceedings of the IEEE/CVF Conference on Computer Vision and Pattern Recognition*, pages 1512–1521, 2021. [2, 7](#)
- [12] David Lopez-Paz, Léon Bottou, Bernhard Schölkopf, and Vladimir Vapnik. Unifying distillation and privileged information. *arXiv preprint arXiv:1511.03643*, 2015. [5, 6](#)
- [13] Seyed Iman Mirzadeh, Mehrdad Farajtabar, Ang Li, Nir Levine, Akihiro Matsukawa, and Hassan Ghasemzadeh. Improved knowledge distillation via teacher assistant. In *Proceedings of the AAAI conference on artificial intelligence*, volume 34, pages 5191–5198, 2020. [5, 6](#)
- [14] Yurii E Nesterov. A method for solving the convex programming problem with convergence rate $o(1/k^2)$. In *Dokl. akad. nauk Sssr*, volume 269, pages 543–547, 1983. [6](#)
- [15] Augustus Odena, Christopher Olah, and Jonathon Shlens. Conditional image synthesis with auxiliary classifier gans. In *International conference on machine learning*, pages 2642–2651. PMLR, 2017. [6](#)
- [16] Adam Paszke, Sam Gross, Francisco Massa, Adam Lerer, James Bradbury, Gregory Chanan, Trevor Killeen, Zeming Lin, Natalia Gimelshein, Luca Antiga, et al. Pytorch: An imperative style, high-performance deep learning library. *Advances in neural information processing systems*, 32, 2019. [6](#)
- [17] Biao Qian, Yang Wang, Hongzhi Yin, Richang Hong, and Meng Wang. Switchable online knowledge distillation. In *Computer Vision–ECCV 2022: 17th European Conference, Tel Aviv, Israel, October 23–27, 2022, Proceedings, Part XI*, pages 449–466, 2022. [1](#)
- [18] Olga Russakovsky, Jia Deng, Hao Su, Jonathan Krause, Sanjeev Satheesh, Sean Ma, Ziheng Huang, Andrej Karpathy, Aditya Khosla, Michael Bernstein, et al. Imagenet large scale visual recognition challenge. *International journal of computer vision*, 115(3):211–252, 2015. [6](#)
- [19] J v. Neumann. Zur theorie der gesellschaftsspiele. *Mathematische annalen*, 100(1):295–320, 1928. [3](#)
- [20] Vladimir Vapnik. *The nature of statistical learning theory*. Springer science & business media, 1999. [5](#)
- [21] Shoukai Xu, Haokun Li, Bohan Zhuang, Jing Liu, Jiezhang Cao, Chuangrun Liang, and Mingkui Tan. Generative low-bitwidth data free quantization. In *European Conference on Computer Vision*, pages 1–17. Springer, 2020. [1, 2, 5, 6, 7, 8](#)
- [22] Xiangguo Zhang, Haotong Qin, Yifu Ding, Ruihao Gong, Qinghua Yan, Renshuai Tao, Yuhang Li, Fengwei Yu, and Xianglong Liu. Diversifying sample generation for accurate data-free quantization. In *Proceedings of the IEEE/CVF Conference on Computer Vision and Pattern Recognition*, pages 15658–15667, 2021. [1](#)
- [23] Yunshan Zhong, Mingbao Lin, Gongrui Nan, Jianzhuang Liu, Baochang Zhang, Yonghong Tian, and Rongrong Ji. Intraq: Learning synthetic images with intra-class heterogeneity for zero-shot network quantization. In *Proceedings of the IEEE/CVF Conference on Computer Vision and Pattern Recognition*, pages 12339–12348, 2022. [7](#)
- [24] Baozhou Zhu, Peter Hofstee, Johan Peltenburg, Jinho Lee, and Zaid Alars. Autorecon: Neural architecture search-based reconstruction for data-free compression. *arXiv preprint arXiv:2105.12151*, 2021. [1, 2, 7](#)